

Vortical laser bullets in femtosecond pulse propagation

Vladimir Mezentsev¹, Mykhaylo Dubov¹,
Alexey Wolf^{2,3}, and Alexander Dostovalov²

¹ Aston Institute for Photonic Technologies, Aston University, Birmingham, UK

² Institute of Automation and Electrometry, Novosibirsk, Russia,

³ Novosibirsk State University, Novosibirsk, Russia

5th August 2014

What is femtosecond microfabrication

Absorption of energy

Theoretical model

Femtosecond vortex bullets – rings of light

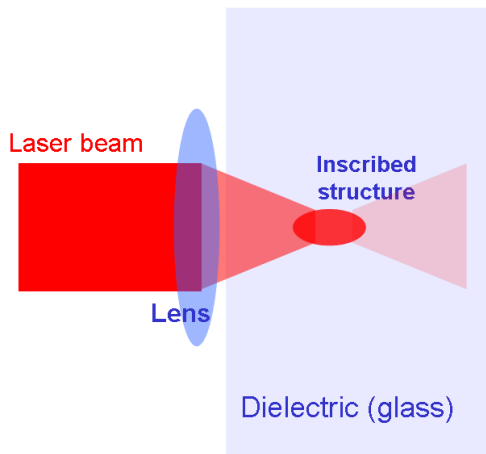
Numerical results

Conclusions

Acknowledgement. This work is being supported by FP7 ISIS collaboration project between Aston and Novosibirsk.

Principle of femtosecond (fs) microfabrication

femtosecond microfabrication for dummies i.e. theoreticians



Laser pulse enters left to right

Energy deposition estimation

Absorption of modest energy may produce a lot of damage

Let's consider a fs pulse with energy $E = 1 \mu\text{J}$.

What temperature can be achieved if all this energy is absorbed at focal volume $V = 1 \mu\text{m}^3$?

$$E = C_V \rho_m V \Delta T$$

$$C_V = 0.75 \times 10^3 \text{ J/kg/K}$$

$$\rho_m = 2.2 \times 10^3 \text{ kg/m}^3$$

- ▶ Temperature rise is then estimated as **1,000,000°K**
- ▶ 20X Larger cigar shape of absorption domain **50,000°K**
- ▶ Transparency (only 10–30% of energy is absorbed) **5,000°K**
- ▶ Typically, inscription operates at smaller energies **1,000°K**
- ▶ **Still a lot!!!**

Fs inscription scenario

- ▶ In fs region, there is a remarkable separation of timescales of different processes which makes possible a separate consideration of
 - ▶ Electron collision time < 10 fs
 - ▶ Propagation+ionisation ~ 100 fs
 - ▶ Recombination of plasma ~ 1 ps
 - ▶ Thermoplasticity/densification ~ 1 ms
- ▶ Separation of the timescales allows to treat electromagnetic propagation in the presence of plasma separately from other [very complex] phenomena
- ▶ Plasma density translates to the material temperature as the energy gets absorbed instantly compared to the thermoelastic timescale

Reduced wave equation

[M. D. Feit and J. A. Fleck, Appl. Phys. Lett., 1974]

Extended Non-Linear Schrödinger Equation (NLSE)
for envelope amplitude of electric field

$$i\mathcal{E}_z + \frac{1}{2k}\Delta_{\perp}\mathcal{E} - \frac{k''}{2}\frac{\partial^2\mathcal{E}}{\partial t^2} + k_0n_2|\mathcal{E}|^2\mathcal{E} = \\ - \frac{i\sigma}{2}(1 + i\omega\tau)\rho\mathcal{E} - i\frac{\beta^{(K)}}{2}|\mathcal{E}|^{2(K-1)}\mathcal{E}$$

Electron balance equation for electron concentration:

$$\frac{\partial\rho}{\partial t} = \frac{1}{n_b^2}\frac{\sigma_{bs}}{E_g}\rho|\mathcal{E}|^2 + \frac{\beta^{(K)}}{K\hbar\omega}|\mathcal{E}|^{2K}$$

$K = E_g/\hbar\omega$, $K = 5, 6$ for $\lambda = 800$ nm in fused silica;
 $K = 2$ for $\lambda = 267$ nm = $800/3$ nm.

Physical parameters (fused silica, $\lambda = 800$ nm)

Dispersion

$$k'' = \partial^2 k(\omega) / \partial \omega^2 = 361 \text{ fs}^2 / \text{cm GVD coefficient}$$

Kerr effect

$$n_2 = 3.2 \times 10^{-16} \text{ cm}^2 / \text{W nonlinear refraction index}$$

Plasma absorption (inverse Bremsstrahlung)

$$\sigma = (k / \rho_{BD}) \times \omega \tau / (1 + \omega^2 \tau^2) = 2.78 \times 10^{-18} \text{ cm}^2$$

$\tau \sim 1$ fs — the shortest electron collision time

Multi-Photon Absorption (MPA)

$$\beta_K = \hbar \omega \sigma_K \rho_a - \text{MPA coefficient}$$

$$\sigma_K = 1.3 \times 10^{-55} (\text{cm}^2 / \text{W})^K / \text{s}$$

$$E_g = 7.5 \text{ eV} - \text{ionisation energy}$$

Physical parameters (cont.)

$$\rho_a = 2.1 \times 10^{22} \text{ cm}^{-3} \text{ — atom concentration}$$

$$\rho_{BD} = \varepsilon_0 m_e e^{-2} \omega^2$$

— Break Down (BD) plasma concentration is determined from the condition

$$\omega = \omega_p = \sqrt{\frac{\rho e^2}{\varepsilon_0 m_e}}$$

$$\rho_{BD} = 1.7 \times 10^{21} \text{ cm}^{-3} \text{ for } 800 \text{ nm}$$

Estimation of the inscription threshold

Electron balance equation

$$\frac{\partial \rho}{\partial t} = \frac{1}{n_b^2} \frac{\sigma_{bs}}{E_g} \rho |\mathcal{E}|^2 + \frac{\beta^{(K)}}{K \hbar \omega} |\mathcal{E}|^{2K}$$

can be presented in normalised form by introducing scales ρ_{BD} for ρ and t_p for t :

$$\frac{\partial \rho}{\partial t} = \frac{1}{n_b^2} \frac{\sigma_{bs}}{E_g} \rho |\mathcal{E}|^2 + \frac{\rho_{BD}}{t_p} \left(\frac{I}{I_{MPA}} \right)^K ;$$

$$I_{MPA} = \left(\frac{K \hbar \omega \rho_{BD}}{t_p \beta_K} \right)^{1/K} \sim 25 \times 10^{12} \text{W/cm}^2 !!!$$

– naturally introduced intensity threshold for ionisation.
It is seen that ionization kicks off when intensity exceeds the threshold I_{MPA}

Evolution of energy. Fundamental identity

For the pulse energy

$$E(z) = \int_0^{\infty} 2\pi r dr \int_{-\infty}^{\infty} I(z, r, t) dt ; \quad I = |\mathcal{E}|^2$$

the wave equation holds the identity

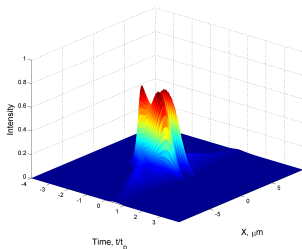
$$\frac{dE(z)}{dz} = - \int_0^{\infty} 2\pi r dr \int_{-\infty}^{\infty} dt \left(\sigma \rho I + \beta^{(K)} I^K \right)$$

A big question:

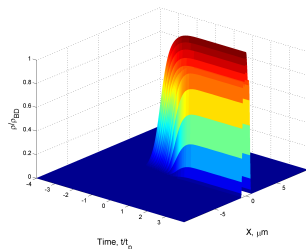
How to determine evolution of intensity $I(z, r, t)$?

Numerical modelling is used to determine $I(z, r, t)$

What is left behind the laser pulse



Light intensity pattern



Plasma pattern

Laser pulse leaves behind a stationary cloud of plasma described by asymptotic distribution of plasma concentration:

$$\rho(\mathbf{r}, z) = \int_{-\infty}^{\infty} \left[\frac{1}{n_b^2} \frac{\sigma}{E_g} \rho |\mathcal{E}(\mathbf{r}, z, t)|^2 + \frac{\beta^{(K)}}{K \hbar \omega} |\mathcal{E}(\mathbf{r}, z, t)|^{2K} \right] dt .$$

Low energy case

$$i\mathcal{E}_z + \frac{1}{2k}\Delta_{\perp}\mathcal{E} - \frac{k''}{2}\frac{\partial^2\mathcal{E}}{\partial t^2} + k_0n_2|\mathcal{E}|^2\mathcal{E} = \\ - \frac{i\sigma}{2}(1+i\omega\tau)\rho\mathcal{E} - i\frac{\beta^{(K)}}{2}|\mathcal{E}|^{2(K-1)}\mathcal{E}$$

For low pulse energies when peak intensity is below 10 TW/cm² there is no absorption. Moreover the dispersion is also negligible at the propagation distances below the dispersion length of 5 mm for 100 fs pulses.

Hence low energy pulses can be accurately described by the stationary NLSE:

$$i\mathcal{E}_z + \frac{1}{2k}\Delta_{\perp}\mathcal{E} + k_0n_2|\mathcal{E}|^2\mathcal{E} = 0$$

Typical initial conditions

Typically, the Gaussian initial condition is being used:

$$\mathcal{E}(z = 0, r, t) = \sqrt{\frac{2P_{in}}{\pi r_0^2}} \exp\left(-\frac{r^2}{r_0^2} - \frac{ikr^2}{2f} - \frac{t^2}{t_p^2}\right),$$

r_0 is the waist of the incident beam

t_p defines the conventionally defined pulsewidth

$$t_{FWHM} = \sqrt{2 \ln 2} t_p \approx 1.177 t_p$$

f is a focal length of the objective lens.

$P_{cr} = \lambda^2 / (2\pi n n_2) \sim 2.3$ MW critical power for self-focusing

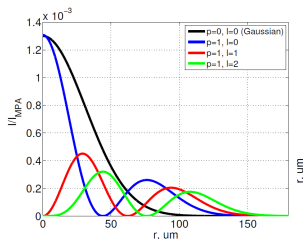
Light bullet laser pulse limited in space and time

Vortical laser bullets

The linear modes of the LSE are Gauss-Laguerre (GL) modes which are used to form a modified initial condition with a vortex built in:

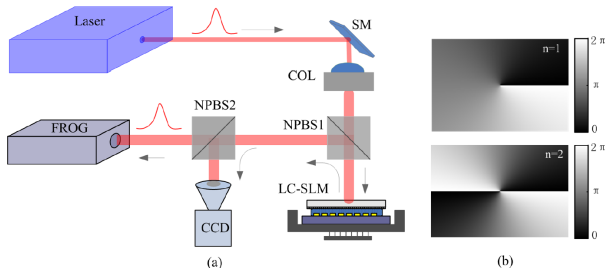
$$\mathcal{E}(r, \phi, z = 0) = \sqrt{\frac{2P_{in}}{\pi r_0^2}} \left(\frac{\sqrt{2}r}{r_0}\right)^{|m|} L_p^m\left(\frac{2r^2}{r_0^2}\right) \exp\left(-\frac{ikr^2}{2f} + im\phi\right),$$

where the quantum numbers p and m enumerate different orders of the radial and azimuthal modes.



Radial profiles of the first few GL modes

Experimental implementation of optical vortex with a phase plate



a) Experimental setup for characterisation of vortex beams. Phase plate is implemented with LC-LSLM (Liquid Crystal Spatial Light Modulator). b) Phase plates for 2π and 4π angular phase modulation.

Equations for numerics

$$i\mathcal{E}_z + \frac{1}{2k}\Delta_{\perp}\mathcal{E} - \frac{k''}{2}\frac{\partial^2\mathcal{E}}{\partial t^2} + k_0n_2|\mathcal{E}|^2\mathcal{E} = \\ - \frac{i\sigma}{2}(1+i\omega\tau)\rho\mathcal{E} - i\frac{\beta^{(K)}}{2}|\mathcal{E}|^{2(K-1)}\mathcal{E}$$

In cylindrical geometry z, r, ϕ one can express the transverse Laplacian as

$$\Delta_{\perp} = \frac{1}{r}\frac{\partial}{\partial r}r\frac{\partial}{\partial r} + \frac{1}{r^2}\frac{\partial^2}{\partial\phi^2}$$

We look for evolution of the vortex-type solutions with the angular symmetry

$$\mathcal{E} = A(z, r, t)e^{im\phi},$$

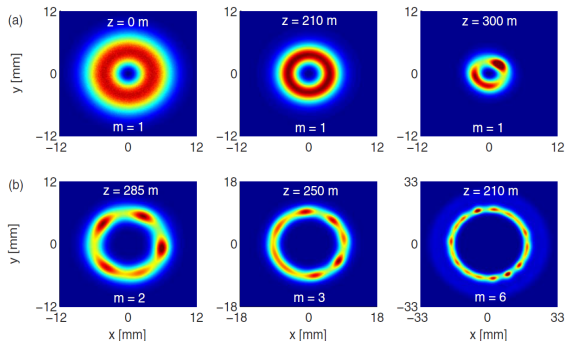
so that the transverse Laplacian becomes a radially symmetric operator

$$\Delta_{\perp} = \frac{1}{r}\frac{\partial}{\partial r}r\frac{\partial}{\partial r} - \frac{m^2}{r^2}$$

Necklace instability

Femtosecond Optical Vortices in Air

[Vincotte, Berge, PRL, 2005]



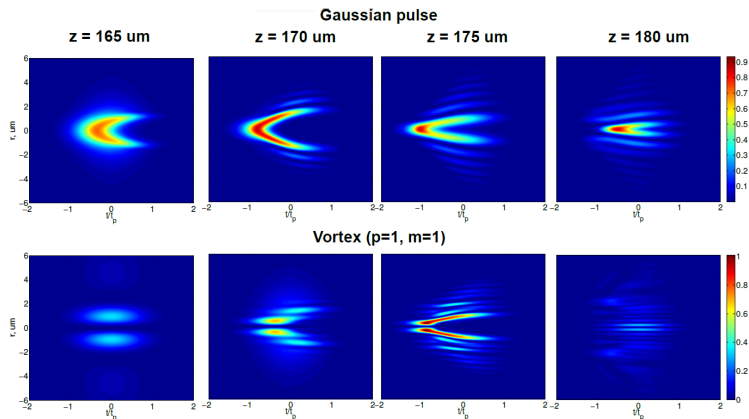
Azimuthal break up of bright vortices (necklace instability for different angular charges m).

$P_{in} = 9P_{CR}$ for $m = 1$, $P_{in} = 17.9P_{CR}$ for $m = 2$,

$P_{in} = 28.7P_{CR}$ for $m = 3$, and $P_{in} = 69.6P_{CR}$ for $m = 6$

Numerical results

Comparison of the light intensity patterns

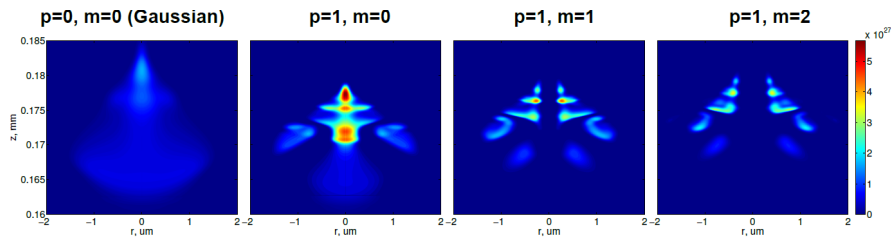


Top row: evolution of the Gaussian light bullet

Bottom row: the same for the vortex bullet with $m = 1, p = 1$ and the same energy.

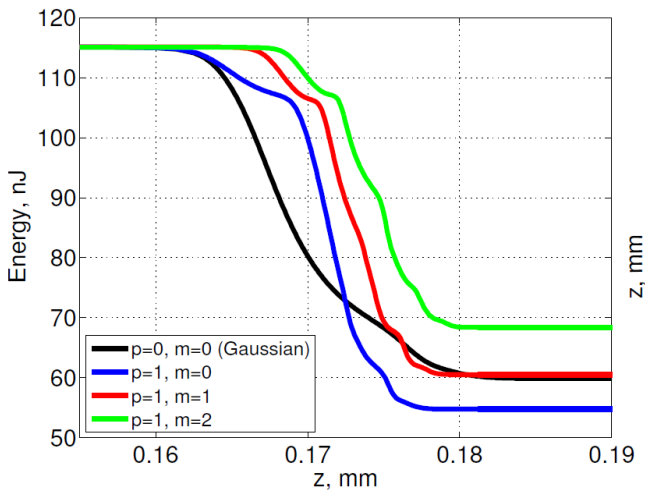
Numerical results

Comparison of the plasma patterns



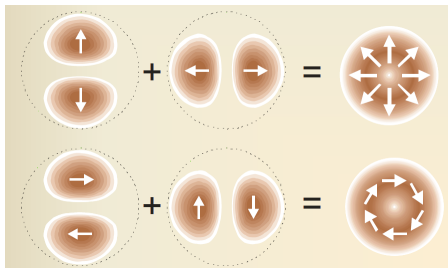
Plasma clouds produced by the femtosecond pulses of the same energy but with different angular charges.

Evolution of pulse energy



Evolution of the pulse energy versus propagation distance for different vortex bullets

Mixed (inhomogeneous) polarization



Linear superposition of orthogonal polarisation states lead to other useful beams with even more intricate polarisation patterns.

However nonlinear analysis becomes more involved. Most likely, the coupled extended NLSE is required in this case

Conclusions

- ▶ Numerical modelling of axially symmetric optical vortex beams has been performed
- ▶ It was found that the laser-plasma dynamics is much more intricate in vortical configurations compared to the plain Gaussian beams.
- ▶ It turns out that the focusing and absorption of the vortex-shaped femtosecond pulses lead to creation of rings followed by compact needle-like structures which are more compact compared to those produced with Gaussian beams.
- ▶ The laser energy deposition in terms of nonlinear absorption is more efficient for vortex-shaped beams.